# Self-consistent full-band Monte Carlo device simulation for strained nMOSFETs incorporating vertical quantization, multi-subband, and different channel orientation effects

Masami Hane, Takeo Ikezawa*, Michihito Kawada*, Tatsuya Ezaki** and Toyoji Yamamoto

System Devices Research Laboratories, NEC Corporation
1120 Shimokuzawa, Sagamihara 229-1198, Japan,     E-mail: hane@az.jp.nec.com
*NEC Informatec Systems, Ltd.     **Hiroshima University

*Abstract*—Strain effects on different crystallographic channel silicon nMOSFETs have been investigated by using a self-consistent quantum mechanical full-band (multi-subband) Monte Carlo (MC) device simulation. Simulation results show that the nMOSFET drain-current increases with applying uniaxial tensile stress while it exhibits different behavior for <100> and <110> different channel directions. Further detailed analyses have been made to clarify appropriate physical mechanism of the drive-current-increase by means of a source-side-injection/ backscattering concept.

*Keywords-device simulation; Monte Carlo; strained MOSFETs; multi-subband; channel orientation*

## I.     INTRODUCTION

Recently, a strain engineering and understanding its mechanism are becoming increasingly important for driving further technological scaling. From such the strain engineering aspect, a selection of channel crystal orientation is particularly interesting.

Regarding nMOSFETs, for instance, very recent experimental observations [1,2] show some contradicted arguments: uniaxial strained bulk-Si mobility of <110> becomes higher than that of <100> under high tensile stress condition [1] while a strained Si-MOSFET with SiC-S/D exhibited higher drain-current for <100> channel orientation [2].

Some simple theoretical analysis of mobility or ideal ballistic current may not be sufficient for deeper understanding of the complicated small-sized MOSFET behavior where the surface-quantization and source-injection/backscattering effects play significant role for the drain-current ($I_{DS}$).

Previous device simulation attempts, however, did not provide appropriate analysis, e.g. like a full-band MC simulation without quantization [3] or a multi-subband MC modeling [4] that might be powerful however no strain issue was given in Ref. 4.

In order to clarify detailed mechanism of strain-effects and enable appropriate strain-engineering for further device performance boost, a new device simulation tool is to be developed considering full-band structure, quantization and strain effects.   In this paper, a full-band Monte-Carlo approach is presented and simulation results of uniaxial-strain effects on nMOSFET with different channel crystal-orientations are presented.
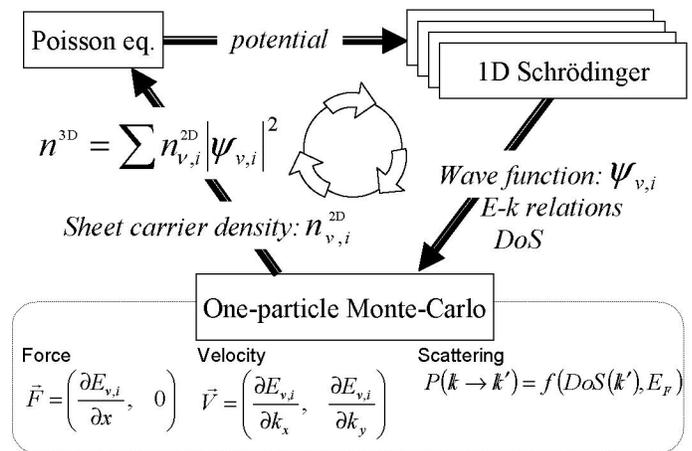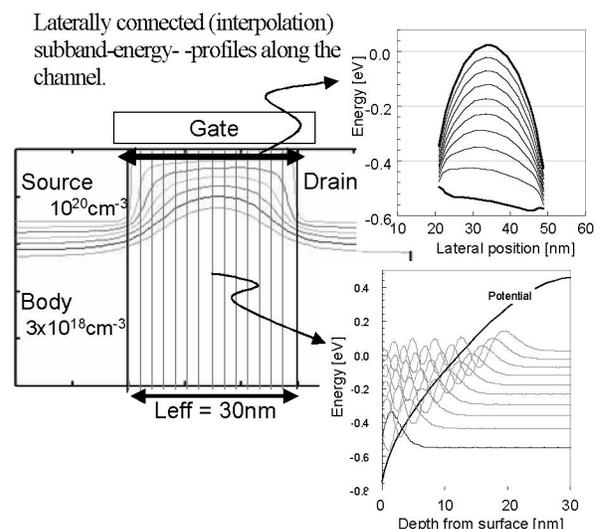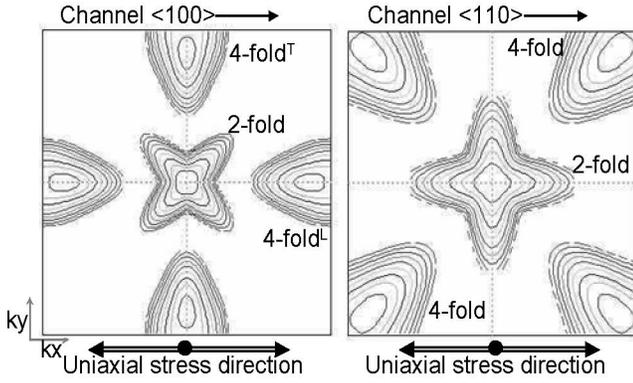


Figure 1.     Simulation flowchart

$$n^{3D} = \sum n_{v,i}^{2D} \left| \psi_{v,i} \right|^2$$

Sheet carrier density: $n_{v,i}^{2D}$

Wave function: $\psi_{v,i}$
E-k relations
DoS

Force
$$\vec{F} = \left( \frac{\partial E_{v,i}}{\partial x}, \quad 0 \right)$$

Velocity
$$\vec{V} = \left( \frac{\partial E_{v,i}}{\partial k_x}, \quad \frac{\partial E_{v,i}}{\partial k_y} \right)$$

Scattering
$$P(k \to k') = f\left(DoS(k'), E_F\right)$$



Figure 2.     Multi-subband calculation example. Schrödinger equations are solved along many vertical slices.

55

## II. MODELING

A new simulation code described here is based on our previous MC modeling approach [5] with extending the approach to consider not only the full-band structure but also multi-subband as self-consistent eigen-solutions of Schrödinger-Poisson (S-P) equations in an iterative scheme as shown in Fig. 1.

Contrary to previously reported method [4,5], strained-silicon full-band structures (Fig. 3) were obtained by using an empirical pseudo-potential method considering a crystal-lattice strain depending applied stress conditions. For a given MOSFET 2D structure and doping profile, a simulation starts from the initial guess of 2D potential provided by a drift-diffusion simulation. Then, along many vertical slices of the MOSFET, 1D S-P equations are solved to obtain multi-subband energy profiles which are to be connected along the lateral-channel-direction by the spline-interpolation as shown in Figs 1-2.



Figure 4.　Calculated surface potential and sheet carrier density.



Figure 3.　Examples of the calculated full-band-structures in kx-ky planes accounting for lattice strain for the strained samples. Silicon lattice strain was calculated applying uniaxial stress $F$ with these material parameters ($C_{11}$, $C_{12}$, and $C_{44}$).

$$T \begin{pmatrix} C_{11} & C_{12} & C_{12} & 0 & 0 & 0 \\ C_{12} & C_{11} & C_{12} & 0 & 0 & 0 \\ C_{12} & C_{12} & C_{11} & 0 & 0 & 0 \\ 0 & 0 & 0 & C_{44} & 0 & 0 \\ 0 & 0 & 0 & 0 & C_{44} & 0 \\ 0 & 0 & 0 & 0 & 0 & C_{44} \end{pmatrix} T^{-1} \begin{pmatrix} \varepsilon_{xx} \\ \varepsilon_{yy} \\ \varepsilon_{zz} \\ 2\varepsilon_{yz} \\ 2\varepsilon_{zx} \\ 2\varepsilon_{xy} \end{pmatrix} = \begin{pmatrix} F_{xx} \\ F_{yy} \\ F_{zz} \\ F_{yz} \\ F_{zy} \\ F_{xy} \end{pmatrix} = \begin{pmatrix} F \\ 0 \\ 0 \\ 0 \\ 0 \\ 0 \end{pmatrix}$$

$C_{11}$ = 167.4GPa　　T: Rotation Matrix
$C_{12}$ = 65.23GPa　　$\varepsilon_{ij}$: Strain tensor
$C_{44}$ =79.57GPa　　$F_{ij}$: Stress tensor

Carrier-transport, i.e. drain-current is calculated by using one-particle MC scheme where the 2D-gas electrons are set both in source and drain thermally (from Density-of-States and Fermi-Dirac distribution function) and then forced to move
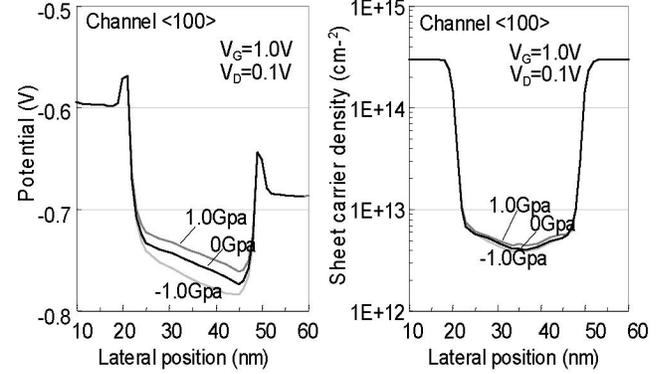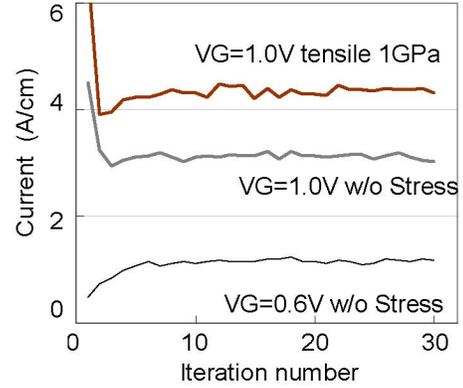


Figure 5.　Drain current as a function of iteration count, representing convergence behavior. Typically one-bias-point takes about 10 hours of CPU-time.

according to each subband-energy differential ($dEv,i/dx$) [4, 5]. In this work, an acoustic phonon scattering effect was taken into account with Pauli's exclusion principle considered [6]. many samplings of one-particle MC are performed that gives a new sheet carrier density profile which is to be expanded to the 3D carrier density distribution profile using all the wave-function, then 2D Poisson equation is solved to update a new 2D potential profile. These procedures should be iterated until convergence is reached (Fig. 5). We applied this new device simulation to uniaxially strained Lg=30nm planer bulk nMOSFET on {100} surface aligned for <100> or <110> channel orientation.

## III. RESULTS AND DISCUSSION

Calculation results for on-current ($I_{DS}$) under various uniaxial stress conditions were shown in Fig. 6. Figure 7 also shows calculated on-current gain as a function of applied stress values.

These simulation results show that $I_{DS}$ increased with increasing uniaxial stress up to 2Gpa for <110> while saturated for <100> as shown in Fig. 7. This result seems to be consistent with the

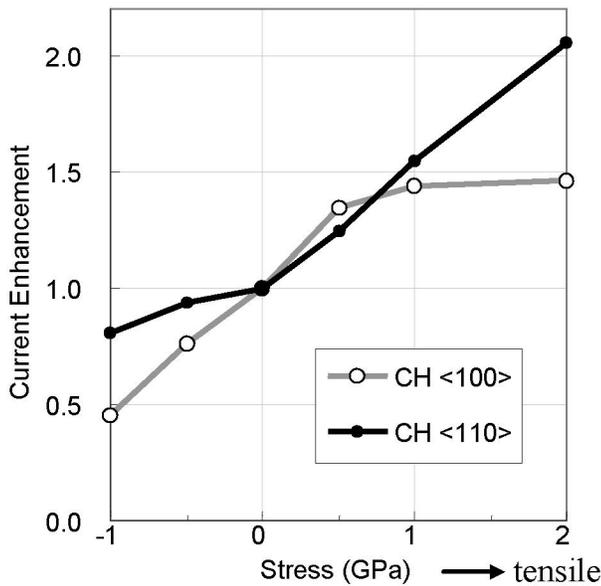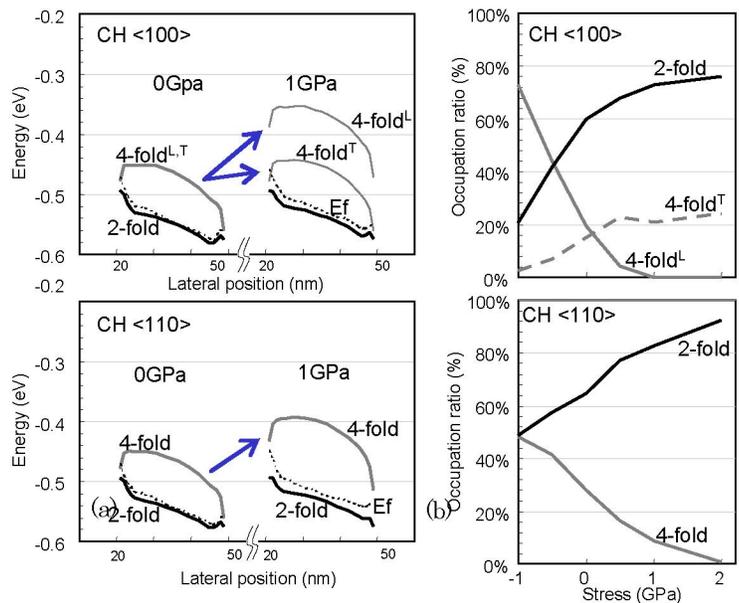Figure 6. Calculation results for $V_G$-$I_{DS}$ for <100> channel MOSFETs under some stress conditions.



Figure 8. (a) Band energy profiles for the lowest subband of each valleys, (b) Band occupation ratio for each valleys as a function of applied stress. Ending-up for the 4-fold (longitudinal) valley occupation explains Fig.7 behavior of early saturation for <100> channel strained-devices.

These particular strain-induced effects can be generously explained by the higher occupation ratio of the 2-fold to 4-fold valleys with increased energy-level-splitting where 2-fold and half-of-4-fold valleys are mostly occupied for <100> and the occupation will be emptied for the other half of 4-fold valleys for applying higher-stress, while in the <110> case $I_{DS}$ increases until the 4-fold valley occupation is completely ended-up up to 2Gpa applied as shown in Fig. 8.

Our Monte Carlo device simulation helps us to understand these particular results of the strain-induced effects by means of a source-side injection/backscattering concept of the MOSFET drive-current, i.e. $I_{DS} = n \cdot V_{inj} \cdot (1-R)/(1+R)$, where $n$ represents number of electrons in the source, $V_{inj}$ represents an average thermal velocity in the source which is evaluated here as the initial velocity for one-particle MC part taking the sampling from the Density-of-States in the source-end in conjunction with Fermi-Dirac function, thus regarded as *source-side injection velocity* in this simulation, and *(1-R)* term represents a channel injection efficiency associated with a backscattering rate $R$. According to our simulation results for applying higher tensile stress, $I_{DS}$ increased 150-200% overall.

Relative $V_{inj}$ and $R$ contributions are interesting rather than source-side $n$. The simulation analysis shows that the relative increase of $V_{inj}$ with the higher stress becomes about 125% as shown in Fig. 9. The rest of the relative contribution *(1-R)/(1+R)* should be over 160% in order to give the net 200% gain. The scattering contribution was evaluated separately in detail by



Figure 7. $I_{DS}$ enhancement as a function of uniaxial tensile stress. <100> channel $I_{DS}$ saturates earlier than <110> case (being consistent with Ref.1)

experimental argument presented in Ref. 1. Meanwhile, below 1 Gpa, $I_{DS}$ for <100> becomes somewhat higher than that for <110>, and it also seems to be consistent with the <100> preference argued in Ref. 2.

extracting mean-free-path $\lambda_0$ within the $kT$-layers, and also by examining direct samplings of backward-particle-counts within the lowest subband from this simulation results. The backscattering ratio $R_{scat}$, derived from $\lambda_0$ (averaged for all the sub-bands), was found to be decreased with increasing tensile stress as shown in Fig. 10. It was found that the phonon scattering plays the role mostly, but also the backward motions relevant to the upper sub-band profiles can not be fully neglected to evaluate the net $R$.
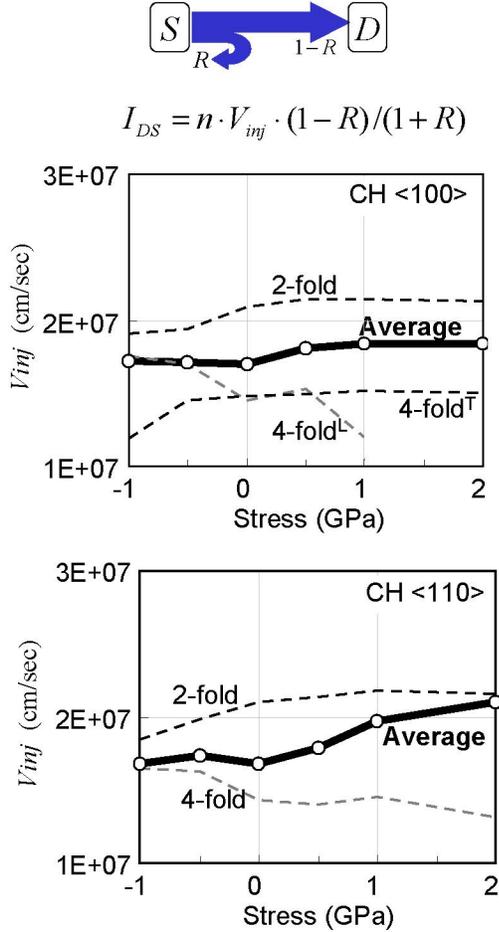
$$I_{DS} = n \cdot V_{inj} \cdot (1-R)/(1+R)$$



Figure 9. Extracted $V_{inj}$ (source-side thermal velocity considering Fermi-Dirac statistics)



Figure 10. Backscattering component as a function of applied stress, derived from mean-free-path with a formula of [ $R_{scat}=1/(1+\lambda_0/l_{kT})$ ], (b) Direct sampling results of backscattering ratio in the lowest subband of 2-fold valleys.

Table 1. Contribution ratio of each component for $I_{DS}$ enhancement with 2Gpa tensile stress applied shown in Fig. 7.

|  | Ch <100> | Ch <110> |
|---|---|---|
| $\Delta I_{DS}$ | 146% | 205% |
| $\Delta Vinj$ | 109% | 125% |
| $\Delta[(1-R)/(1+R)]$ | 134% | 164% |
| $\Delta R_{scat}$ | 86% | 77% |

## IV. CONCLUSION

A newly developed quantum mechanical full-band Monte Carlo device simulator which can handle strain effects enables us performing detailed-analysis of strain-induced drive-current change depending on channel crystal-orientation, thereby becoming useful for further device performance optimization toward the next technology generation and beyond.
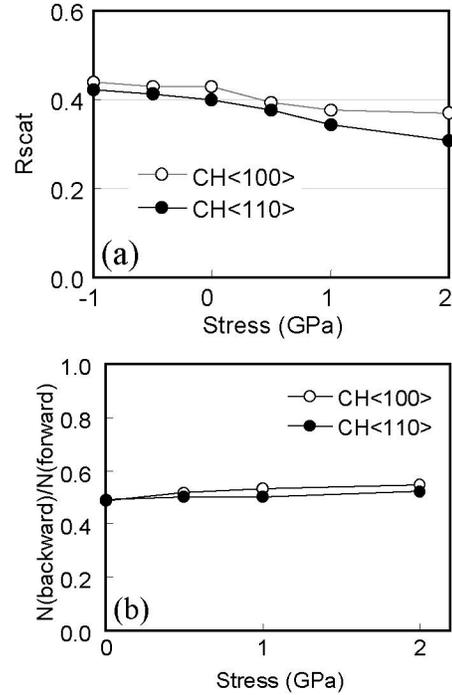
REFERENCES

[1] K. Uchida et al., IEDM Tech. Digs., p.135 (2005)

[2] K.-W. Ang et al., IEDM Tech. Digs., p.503 (2005)

[3] F.M. Bulfer and W. Fichtner, IEEE Trans. Electron Devices, 50, p.278 (2003)

[4] L. Lucci et al., IEDM Tech. Digs, p.631 (2005)

[5] T. Ezaki et al., J. Comp. Elec. 2, p.97 (2003)

[6] T. Ezaki et al., Proc. of SISPAD, p.53 (2004)